

Electron Scattering with Polarized Targets at TESLA

The TESLA-N Study Group ^{*}

M. Anselmino^m, E.C. Aschenauer^e, S. Belostotski^k, W. Bialowons^d,
J. Blümlein^e, V. Braun^l, R. Brinkmann^d, M. Düren^b, F. Ellinghaus^e,
K. Goeke^c, St. Goertz^c, A. Gute^f, J. Harmsen^c, D. v.Harrachⁱ,
R. Jakob^o, E.M. Kabussⁱ, R. Kaiser^e, V. Korotkov^e, P. Kroll^o,
E. Leader^h, B. Lehmann-Dronke^l, L. Mankiewiczⁿ, A. Meier^c,
W. Meyer^c, N. Meyners^d, D. Müller^l, P.J. Mulders^a, W.-D. Nowak^e,
L. Niedermeier^l, K. Oganessyan^d, P.V. Pobilitza^c, M.V. Polyakov^c,
G. Reicherz^c, K. Rith^f, D. Ryckbosch^g, A. Schäfer^l, K. Sinram^d,
G. v.d.Steenhoven^j, E. Steffens^f, J. Steijger^j, C. Weiss^c

^a*Free University Amsterdam*

^b*University of Bayreuth*

^c*Ruhr-University Bochum*

^d*DESY Hamburg*

^e*DESY Zeuthen*

^f*University of Erlangen-Nürnberg*

^g*University of Gent*

^h*Imperial College, London*

ⁱ*University of Mainz*

^j*NIKHEF Amsterdam*

^k*University of St.Petersburg*

^l*University of Regensburg*

^m*INFN Torino*

ⁿ*Nicolaus Kopernicus Astronomical Center Warsaw*

^o*University of Wuppertal*

* Contact: Wolf-Dieter.Nowak@desy.de

Abstract

Measurements of polarized electron-nucleon scattering can be realized at the TESLA linear collider facility with projected luminosities that are about two orders of magnitude higher than those expected of other experiments at comparable energies. Longitudinally polarized electrons, accelerated as a small fraction of the total current in the e^+ arm of TESLA, can be directed onto a solid state target that may be either longitudinally or transversely polarized. A large variety of polarized parton distribution and fragmentation functions can be determined with unprecedented accuracy, many of them for the first time. A main goal of the experiment is the precise measurement of the x - and Q^2 -dependence of the experimentally totally unknown quark transversity distributions that will complete the information on the nucleon's quark spin structure as relevant for high energy processes. Comparing their Q^2 -evolution to that of the corresponding helicity distributions constitutes an important precision test of the predictive power of QCD in the spin sector. Measuring transversity distributions and tensor charges allows access to the hitherto unmeasured chirally odd operators in QCD which are of great importance to understand the role of chiral symmetry. The possibilities of using unpolarized targets and of experiments with a real photon beam turn TESLA-N into a versatile next-generation facility at the intersection of particle and nuclear physics.

Contents

1	Introduction	3
2	Physics Prospects	5
2.1	Transversity Distributions	5
2.2	Helicity Distributions	9
2.3	Polarized Gluon Distribution	10
2.4	Higher Twist	12
2.5	Fragmentation Functions	13
2.6	Specific Deuteron Structure Functions	13
3	Layout of the Experiment	14
3.1	Polarized Target	14
3.2	Polarized Electron Beam	14
3.3	Overview of the Apparatus	16
3.4	Luminosity and Acceptance	18
3.5	Resolution in Kinematic Variables	20
3.6	Civil Engineering	21
4	Summary	22
	References	23

1 Introduction

Today there is widespread confidence that Quantum Chromodynamics (QCD) is the correct theory of strong interactions. On the level of unpolarized parton distribution functions the theory has been tested with considerable precision by many experiments. However, after 10 years of intense theoretical and experimental activities in studying the *polarized* nucleon, the angular momentum composition of the nucleon remains a territory with blank spots. High precision data in a large kinematic domain are required to fully explore the spin structure of QCD.

Measurements of polarized deep-inelastic scattering (DIS) were up to now mostly performed with longitudinally polarized nucleons. Hence, the majority of experimental information on the angular momentum composition of the nucleon is restricted to its longitudinal spin structure. This is characterized through the helicity distributions $\Delta q(x, Q^2)$ (also known as longitudinal quark spin distributions), where q denotes the quark flavor, the ‘Bjorken-variable’ x is the fraction of the nucleon momentum carried by the interacting parton and Q^2 is the virtuality of the exchanged photon. However, of equal importance for a complete understanding of the spin structure of the nucleon as seen in high-energy processes, are the hitherto unmeasured transversity distributions $\delta q(x, Q^2)$, which can only be measured with transversely polarized nucleons.

While a weighted sum of the helicity distributions $\Delta q(x, Q^2)$ is directly accessible in inclusive deep-inelastic scattering (DIS) as the longitudinal spin structure function $g_1(x, Q^2)$, the transversity distributions $\delta q(x, Q^2)$ do not appear in an inclusive structure function. They can, however, be measured in semi-inclusive DIS processes which implies a substantially higher experimental effort. In comparison, the perspectives of RHIC for a direct measurement of transversity are not good [1].

First results on transversity distributions can be expected from HERMES [2] and COMPASS [3] within 3-5 years from now, while a complete high precision mapping of their x - and Q^2 -dependence requires high statistics measurements that are beyond the scope of presently or soon running experiments.

An important reason for the interest in the transversity distributions and their first moments, the tensor charges, is the fact that these quantities are related to matrix elements of chirally odd operators in QCD [4]. All known low-energy probes of hadrons such as electromagnetic or weak currents are chirally even, so that low-energy experiments cannot provide any information about chirally odd matrix elements². Inclusive DIS at large Q^2 (both unpolarized and polarized) measures only chirally even operators, hence a whole class of operators so far remained unmeasured because of the lack of suitable ‘natural’ probes coupling to them. Hadrons are expected to react very differently to chirally odd probes as compared to chirally even ones; e.g. the coupling of the flavor non-singlet tensor charge to pions is completely different from that of the axial charge [5]. A measurement of the transversity distributions and tensor charges would for the first time provide an opportunity to access the ‘missing’ chirally odd operators. In this way it would greatly improve the understanding of the role of chiral symmetry in shaping the structure of the QCD ground state and of the low-mass hadrons.

² An exception is the so-called sigma term, whose effect on hadrons is, however, proportional to the small current quark masses.

The successful understanding and use of *unpolarized* distribution and fragmentation functions in various processes have given confidence that QCD can be used not only for the extension to polarized functions. Moreover, it is also applicable for contributions of higher orders in the coupling constant α_s or beyond leading order in an expansion in the inverse hard scale (Q for deep-inelastic leptonproduction), which is referred to as higher twist. Progress in these directions requires to develop new calculational techniques as well as novel methods to solve the evolution equations associated. These more involved aspects of QCD are just those that are perceived by many theorists to be the most interesting ones. It is widely accepted that QCD is rich enough as a theory to be able to generate the entire hadron and nuclear physics phenomenology. One crucial aspect, however, for most of the relevant physics, namely a complete and systematic control of all relevant higher-order and higher-twist contributions is still not in reach. Straightforward QCD perturbation theory often only converges for some limited kinematic configurations. This is in striking contrast to the fact that much of the available experimental data is easily interpreted by a combination of leading order perturbative calculations and some ‘intuitive’ power-correction terms. It suggests that for many signals a QCD-description could be pushed down to photon virtualities as low as $Q^2 = 1 \text{ GeV}^2$. High accuracy measurements in this domain will provide definitive tests for higher-order and higher-twist QCD calculations.

To the extent that the focus of hadron physics turns to higher energies and more exclusive reactions, a corresponding move is about to begin from the traditional, somewhat ‘model-oriented’ nuclear physics approach towards real QCD descriptions. Recent theoretical investigations encourage such efforts by strongly pushing the limits of previous QCD-techniques towards a much better description of semi-inclusive and exclusive reactions. This requires an extension of the classification of polarized twist-2 and twist-3 distribution and fragmentation functions plus a realistic phenomenology and more sophisticated hadron wave functions. A great potential to achieve an even deeper understanding of the nucleon structure may arise from a comprehensive, generalized analysis of many different processes based on the new tool of skewed parton distributions (SPDs).

The study of hadron structure has another important facet in that it would supply badly needed input for the interpretation of data from Tevatron and LHC. A better understanding of the interplay between soft and hard contributions in exclusive processes is relevant for the success of the B-factories at hadron colliders. Issues of great importance for the LHC include a better determination of the gluon distribution for the whole range of Bjorken- x as well as a better understanding of isolated photon production, which is an important background for $H \rightarrow \gamma + \gamma$.

Within the nuclear and particle physics communities there exists an increasing conviction in the necessity of a new facility to study polarized lepton-nucleon/nucleus scattering with very high luminosity and a high enough center-of-mass energy to cover a sufficient kinematic domain. This document outlines the TESLA-N project, which would use one arm of the TESLA linear collider at DESY for a polarized electron-nucleon fixed-target experiment. The current discussions about ELFE@DESY, ELFE@CERN, eRHIC, EPIC, or a long-term high-energy option for CEBAF are all variations on the same subject. TESLA-N is a highly competitive and very cost-effective alternative option. Its distinguishing property is the unique combination of large center-of-mass energy and high luminosity.

2 Physics Prospects

The HERMES results that have emerged over the recent past are demonstrating the richness of polarized electron-nucleon physics. The higher energy and the much higher luminosity of TESLA-N are expected to again significantly enlarge the number and variety of observable effects as well as the precision with which they can be studied. Naturally, today a theoretical understanding is only available for a part of this potential. Hence, the following list of topics illustrates rather than exhausts the physics potential of TESLA-N.

Detailed projections for the statistical accuracy attainable in one of the TESLA-N key experiments, the precise measurement of the transversity distributions, are given in the following section. Projections for all other topics are included in the sections following below, whenever available. All given projections are based on an integrated luminosity of 100 fb^{-1} . This represents a conservative estimate for *one* year of data taking (cf. section 3.4).

2.1 Transversity Distributions

The nucleon as a spin 1/2 hadron is characterized by three independent flavor sets of (leading order) quark distributions. The distributions $q(x, Q^2)$ - or $f_1^q(x, Q^2)$ - describe the unpolarized nucleon. The transversity distributions $\delta q(x, Q^2)$ - also referred to as $h_1^q(x, Q^2)$ or sometimes as $\Delta_T q(x, Q^2)$ - as well as the helicity distributions $\Delta q(x, Q^2)$ - also referred to as $g_1^q(x, Q^2)$ - describe aspects of the internal spin structure of the nucleon. One important difference between the latter two lies in their different QCD evolution. In contrast to the helicity distributions, the transversity distributions decouple from gluons. The reason is, that the transversity distributions are chirally odd, involving correlations between left- and righthanded quarks. Since $\Delta q(x, Q^2)$ and $\delta q(x, Q^2)$ describe the quark polarization in longitudinally and transversely polarized nucleons, respectively, they are independent functions. However, in the most naive approximation using non-relativistic quarks $\delta q(x) \approx \Delta q(x)$ can be expected.

The first moments of the distribution functions give particular charges, which are matrix elements of local operators. For the unpolarized distributions the first moments of $q(x, Q^2) - \bar{q}(x, Q^2)$ give the flavor charges. For the helicity distributions the first moments of $\Delta q(x, Q^2) + \Delta \bar{q}(x, Q^2)$ give the axial charges $\Delta q(Q^2)$. The flavor sum of these axial charges, $\Delta \Sigma(Q^2)$, is the longitudinal quark spin fraction whose properties have given rise to all the commotion around the nucleon spin because of its anomalous evolution involving the polarized gluon distribution. The first moments of $\delta q(x, Q^2) - \delta \bar{q}(x, Q^2)$ are called tensor charges $\delta q(Q^2)$; their flavor sum is denoted $\delta \Sigma(Q^2)$. Experimentally nothing is known about the tensor charges, in contrast to the flavor and axial charges. While for the axial charges the nonsinglet combinations can also be measured in low-energy experiments (weak decays), no such experiments are known for the tensor charges. The tensor charges $\delta q(Q^2)$ and their flavor sum $\delta \Sigma(Q^2)$ are valence objects and decouple from gluons and sea quarks. In this respect, the tensor charges are expected to be closer to the non-relativistic limit than the axial charges. This is supported by recent lattice QCD calculations [6,7]. Reference [6] quotes values of $\Delta \Sigma = 0.18 \pm 0.10$ for the longitudinal quark spin fraction and $\delta \Sigma = 0.562 \pm 0.088$ for the quark tensor charge at $Q^2 = 2 \text{ GeV}^2$.

As mentioned previously, the transversity distributions $\delta q(x, Q^2)$ are not accessible in

inclusive measurements, because they are chirally odd and only occur in combinations with other chirally odd objects. In semi-inclusive DIS of unpolarized leptons off transversely polarized nucleons several methods have been proposed to access $\delta q(x, Q^2)$ via specific single target-spin asymmetries:

- (1) An asymmetry that involves $\delta q(x, Q^2)$ in combination with the chirally odd polarized fragmentation function $H_1^{\perp(1)}(z)$ can be extracted from the azimuthal distribution of the produced single hadron [8–12]. This fragmentation function correlates the transverse spin of a quark with a preferred transverse direction for the production of the pion.
- (2) A measurement of the momenta of two leading pions gives access to an asymmetry in which $\delta q(x, Q^2)$ combines with a so-called interference fragmentation function [13–15]. Here the transverse spin of the quark is correlated with the relative transverse momentum between the pions.
- (3) The determination of transverse components of the spin vector of produced Λ particles allows the measurement of an asymmetry where $\delta q(x, Q^2)$ combines with a polarized fragmentation function $H_1(z)$ [16].
- (4) Vector-meson production provides other ways to probe $\delta q(x, Q^2)$ employing polarimetry and azimuthal asymmetries [17,18]. For ρ -production, where the polarimetry involves a pion pair, it is part of the above two-pion production.

Option (1) offers the experimentally most direct access to $\delta q(x, Q^2)$. An appropriately weighted cross-section asymmetry can be expressed as a flavor-sum where each transversity distribution function $\delta q(x, Q^2)$ enters in combination with a hitherto unknown polarized fragmentation function $H_1^{\perp(1)q}(z)$ of the same flavor [10]:

$$A_T(x, Q^2, z) = P_T \cdot D_{nn} \cdot \frac{\sum_q e_q^2 \delta q(x, Q^2) H_1^{\perp(1)q}(z)}{\sum_q e_q^2 q(x, Q^2) D_1^q(z)} \quad (1)$$

Here D_{nn} is the transverse polarization transfer coefficient, P_T is the nucleon's transverse polarization, and $D_1^q(z)$ is the unpolarized quark fragmentation function that recently has attracted renewed interest (cf. section 2.5).

Measurements of different asymmetries in the production of positive and negative pions on proton and deuteron targets ($A_p^{\pi^+}$, $A_p^{\pi^-}$, $A_d^{\pi^+}$, $A_d^{\pi^-}$) allow the simultaneous reconstruction of the shapes of the unknown functions $\delta q(x, Q^2)$ and the ratio $H_1^{\perp(1)}(z)/D_1(z)$. This ratio is considered to be flavor independent in the context of this study. The relative normalization can be fixed through independent measurements of $H_1^{\perp(1)}(z)$, e.g. in e^+e^- experiments. Alternatively, an additional assumption can be used, where one of the possibilities is to relate $\delta q(x)$ to $\Delta q(x)$ at small values of Q^2 . The differences between both are smallest in the region of intermediate and large values of x , hence the normalization ambiguity can be resolved at $x_0 = 0.25$ by assuming [19]:

$$\delta u(x_0, Q_0^2) = \Delta u(x_0, Q_0^2) \quad (2)$$

Measurements of all possible asymmetries, $A_{p,d}^{\pi^+(\pi^-)}$, for $N_{(x,Q^2)}$ points in the (x, Q^2) -plane and for N_z points in z yield $4 \cdot N_{(x,Q^2)} \cdot N_z$ measurements. This must be compared to $4 \cdot N_{(x,Q^2)}$ unknown parameters, corresponding to the quark distributions $\delta u(x, Q^2)$, $\delta d(x, Q^2)$, $\delta \bar{u}(x, Q^2)$, $\delta \bar{d}(x, Q^2)$, and to N_z unknown values of $H_1^{\perp(1)}(z)/D_1(z)$. If kaon

asymmetries are measured in addition, the distributions $\delta s(x, Q^2)$ and $\delta \bar{s}(x, Q^2)$ can be included as well. This defines an overconstrained set of coupled equations which can be solved using a standard minimization procedure.

For the determination of the projected statistical accuracies for future measurements of $\delta q(x, Q^2)$ at TESLA-N reasonable input is required for the unknown functions $\delta q(x, Q^2)$ and $H_1^{\perp(1)}(z)/D_1(z)$. The former ones were assumed to coincide with the GRSV LO parameterization [20] for $\Delta q(x, Q^2)$ at the initial scale of $Q^2 = 0.4 \text{ GeV}^2$ and evolved to higher values of Q^2 using the DGLAP equations for transversity distributions. The resulting distributions approximately obey the Soffer bound [21,22]. All T-odd fragmentation functions are constrained by a sum rule [23] but otherwise hardly known. The ratio of fragmentation functions was modelled by adopting the approach of reference [10] and fitting the parameters to recent HERMES [24] and DELPHI [25] data. These results indicate that the fragmentation function $H_1^{\perp(1)}(z)$ may be quite sizeable. Hadron distributions in semi-inclusive production were obtained using the standard generators LEPTO [26] and JETSET [27].

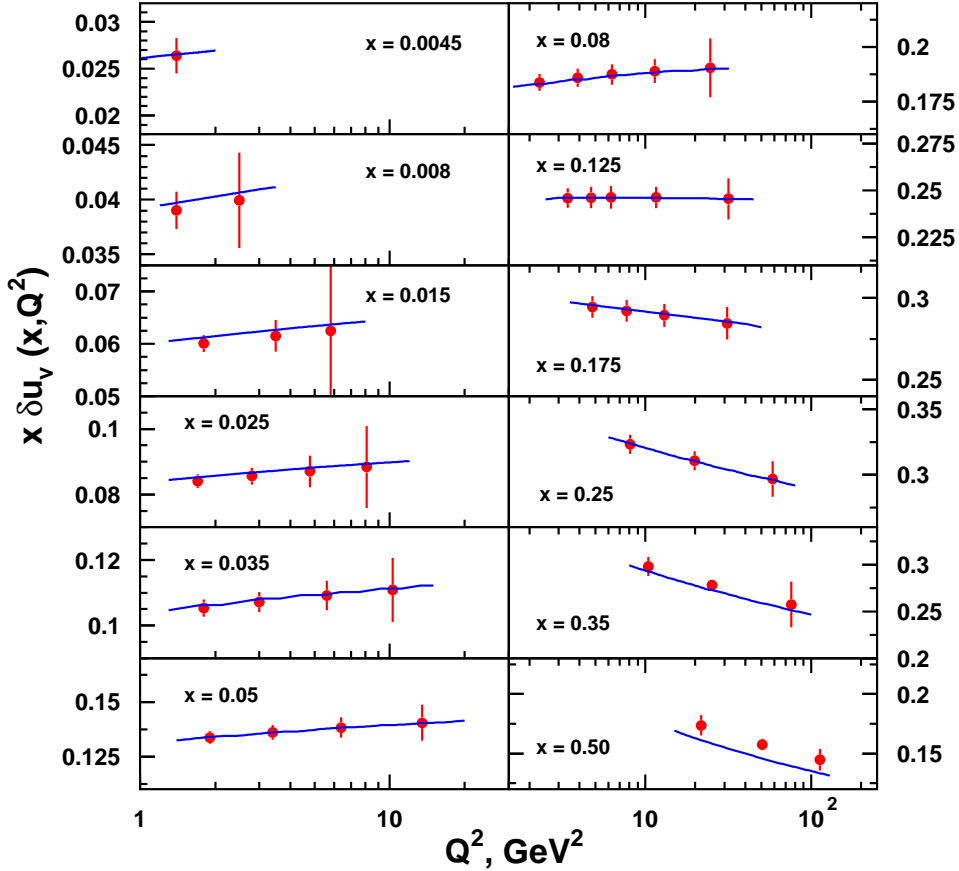


Fig. 1. The valence u -quark transversity distribution as a function of x and Q^2 as it would be measured at TESLA-N, based on an integrated luminosity of 100 fb^{-1} . The curves show the LO Q^2 -evolution of the u_v -quark transversity distribution obtained with a fit to the simulated asymmetries.

The projected statistical accuracy for the measurement of the (x, Q^2) -dependence of the u_v -quark transversity distribution at TESLA-N is shown in figure 1. A broad range of $0.003 < x < 0.7$ can be accessed in conjunction with $1 < Q^2 < 100 \text{ GeV}^2$, with an impressive statistical accuracy over almost the full range. Because of u -quark dominance in pion electroproduction a somewhat lower accuracy is attained in the reconstruction of

the other transversity distributions, δd_v , $\delta \bar{u}$, and $\delta \bar{d}$.

There is a technically different approach to determine the unknown quark distributions and fragmentation function ratios using parameterized transversity distributions. The starting point is a parameter-dependent ansatz for every $\delta q(x, Q_0^2)$, e.g.

$$\delta q(x, Q_0^2) = \eta_q \cdot x^{\alpha_q} (1-x)^{\beta_q} (1 + \gamma_q x + \rho_q \sqrt{x}) \quad (3)$$

at a reference scale Q_0^2 . Here η_q , α_q , β_q , γ_q , and ρ_q are free parameters. These free parameters and the unknown fragmentation function ratios $H_1^{\perp(1)}(z)/D_1(z)$ are fitted to the simulated values of the asymmetries, calculated through eq.(1). In this procedure the distribution functions are evolved in leading order to the necessary Q^2 -values using the above ansatz. The resulting functional dependence for $x \cdot \delta u_v(x, Q^2)$ is represented by the lines drawn in figure 1. In addition, the fit also provides a projection for the accuracy of the tensor charges of u - and d -quarks of 0.88 ± 0.01 and -0.32 ± 0.02 at the scale of 1 GeV^2 , respectively. Note that the absolute values of the tensor charges are defined to a large extent by the input distributions, although the values are rather close to those predicted by lattice QCD calculations. At the same time, the fit yields precise values for the ratio of polarized and unpolarized favored quark fragmentation functions $H_1^{\perp(1)q}(z)/D_1^q(z)$. The projected accuracies, assuming flavor independence, are shown in figure 2.

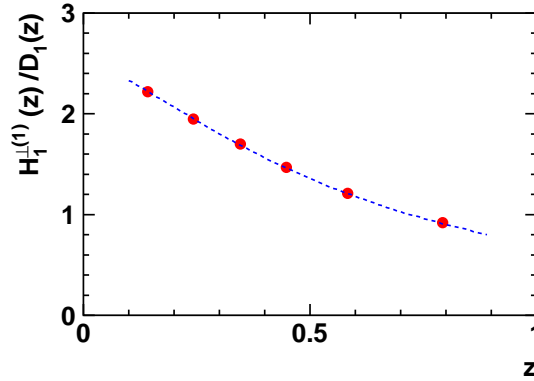


Fig. 2. Projected accuracy of the ratio $H_1^{\perp(1)}(z)/D_1(z)$ of polarized and unpolarized fragmentation functions. The statistical errors are smaller than the point size.

Option (2) (cf. p. 6) focuses on the interference between the s - and p -wave of the two-pion system around the ρ mass. Via the interference effect the polarization information of the quark is contained in $\vec{k}_+ \times \vec{k}_- \cdot \vec{S}_\perp$, where \vec{k}_+ , \vec{k}_- , and \vec{S}_\perp are the three-momenta of π^+ , π^- , and the nucleon's transverse spin, respectively. The corresponding asymmetry depends on the chirally odd $s - p$ wave interference quark fragmentation function $\delta \hat{q}_I(z)$ which is unknown at present, although it can be measured in e^+e^- experiments as well. Theoretically, there is an upper bound for this function that allows the estimation of the maximum possible asymmetry at TESLA-N. The asymmetry is predicted to have different signs below and above the ρ -meson mass. To avoid averaging to zero, it must be considered separately in two regions of the two-pion mass, e.g. $0.51\text{-}0.74 \text{ GeV}$ and $0.78\text{-}0.97 \text{ GeV}$. The corresponding expectations for the asymmetry are shown in figure 3.

At TESLA-N luminosity and kinematic range will be large enough to perform a full flavor separation of both the distribution and the fragmentation functions of the transversely polarized nucleon. This requires measurements of asymmetries in different final states, as well as Q^2 -values that are large enough for factorization to be effective. TESLA-N will meet these requirements.

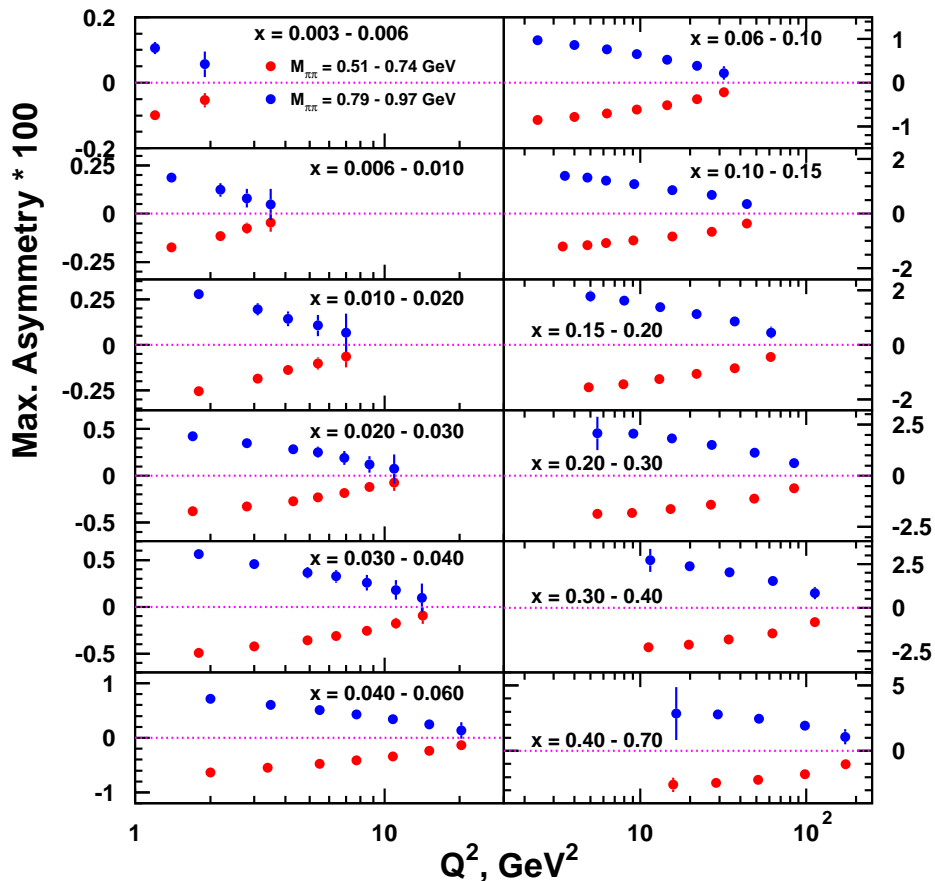


Fig. 3. The maximum asymmetry for the two-pion system as a function of x and Q^2 as it would be measured at TESLA-N with an integrated luminosity of 100 fb^{-1} . Results are shown separately for both two-pion mass regions.

2.2 Helicity Distributions

The luminosity and kinematic range available at TESLA-N will allow the determination of the longitudinal spin structure function $g_1(x, Q^2)$ through inclusive measurements with unprecedented accuracy. The structure function $g_1(x, Q^2)$ represents a particular combination of the helicity distributions Δu , Δd and Δs and the corresponding antiquark distributions. The projection for $g_1^p(x, Q^2)$ is shown in figure 4. The anticipated precision in conjunction with the wide kinematic range will allow studies that so far have not been possible. Prominent examples are the determination of ΔG from NLO fits (cf. section 2.3), higher twist analyses (cf. section 2.4) and a precise determination of the strong coupling constant α_s through the Bjorken sum rule.

SMC [28] and HERMES [29] have provided relevant information on the longitudinally polarized u-quark and d-quark distribution functions. In addition, future HERMES data will allow to constrain $\Delta s(x, Q^2)$, $\Delta \bar{u}(x, Q^2)$ and $\Delta \bar{d}(x, Q^2)$, however, with limited precision. Semi-inclusive measurements with high precision can be provided at TESLA-N, due to the increased luminosity and kinematic range.

For example, a precise measurement of $\Delta \bar{d}(x, Q^2) - \Delta \bar{u}(x, Q^2)$ will strongly influence the picture of the nucleon structure in general. This is the direct parallel to the unpolarized case, where the difference $\bar{d}(x, Q^2) - \bar{u}(x, Q^2)$ was measured to be large. An even larger

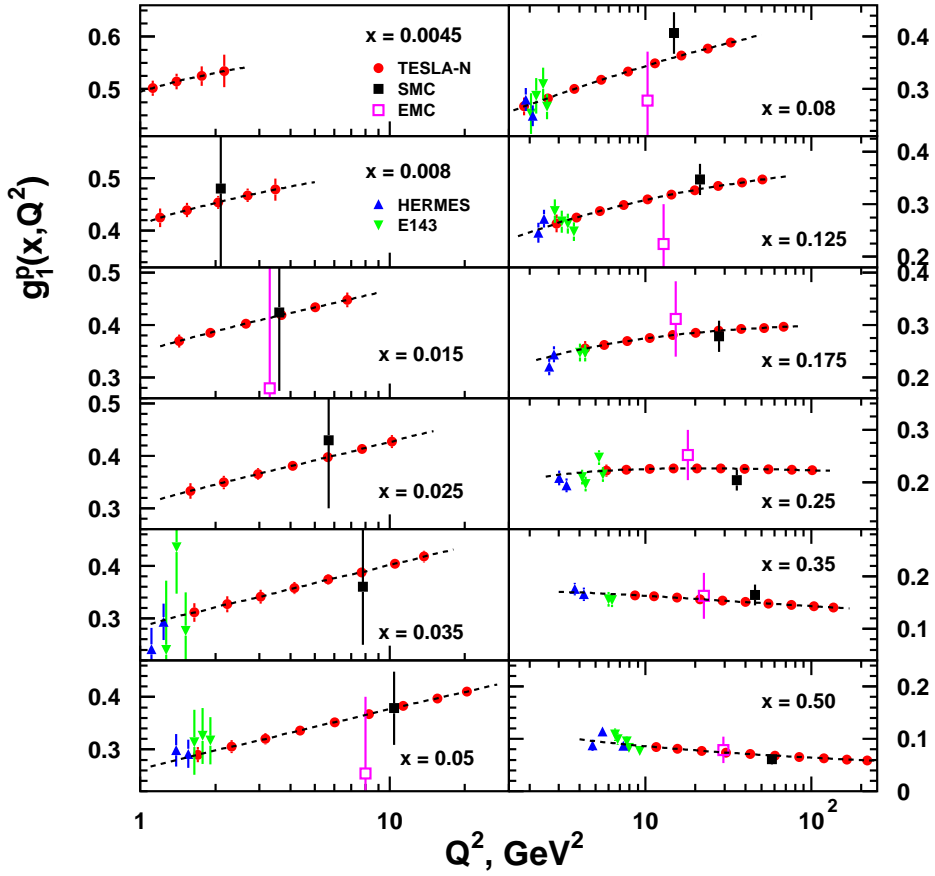


Fig. 4. Projected statistical accuracy for a measurement of $g_1^p(x, Q^2)$ at TESLA-N, based on a luminosity of 100 fb^{-1} and a minimum detector acceptance of 5 mrad. Two EMC/SMC data points are outside of the shown vertical range.

effect is actually predicted for $\Delta\bar{d}(x, Q^2) - \Delta\bar{u}(x, Q^2)$ by e.g. the chiral quark-soliton model [30]. The same holds true for the polarized strange-quark distributions Δs and $\Delta\bar{s}$ which has been an unresolved central issue in the discussion of the nucleon spin structure for more than 10 years.

2.3 Polarized Gluon Distribution

The polarized gluon distribution $\Delta G(x, Q^2)$ of the nucleon is essentially unknown as of today. There is a variety of approaches to determine $\Delta G(x, Q^2)$; the most promising methods in polarized DIS are the analysis of pairs of high- p_\perp hadrons [31], and open charm production [32].

A first indication for the sign and approximate size of $\Delta G(x)$ has already been provided by HERMES through the analysis of quasi-photoproduced pairs of ‘high’- p_\perp hadrons [33]. However, the analysis has to rely on phenomenological event generators, which, due to the limited c.m. energy, are run at the limits of their validity range. The size of the resulting theoretical error is controversial, but it is generally not expected that HERMES can provide a precision measurement of $\Delta G(x)$ along these lines. In contrast, for the considerably higher energies of TESLA-N these problems should be tractable. The anticipated COMPASS results will provide very valuable information, but a high precision experiment

like TESLA-N is eventually needed for a reliable result. At RHIC, the determination of $\Delta G(x)$ is also not without problems in view of the great theoretical uncertainties in direct photon and heavy quark pair production and accounting for the fact that the detectors PHENIX and STAR are optimized for heavy-ion physics. An independent determination in lepton-nucleon scattering is clearly needed to reach solid ground. Up to now, no projections exist for measurements of the Q^2 -dependence of the polarized gluon distribution.

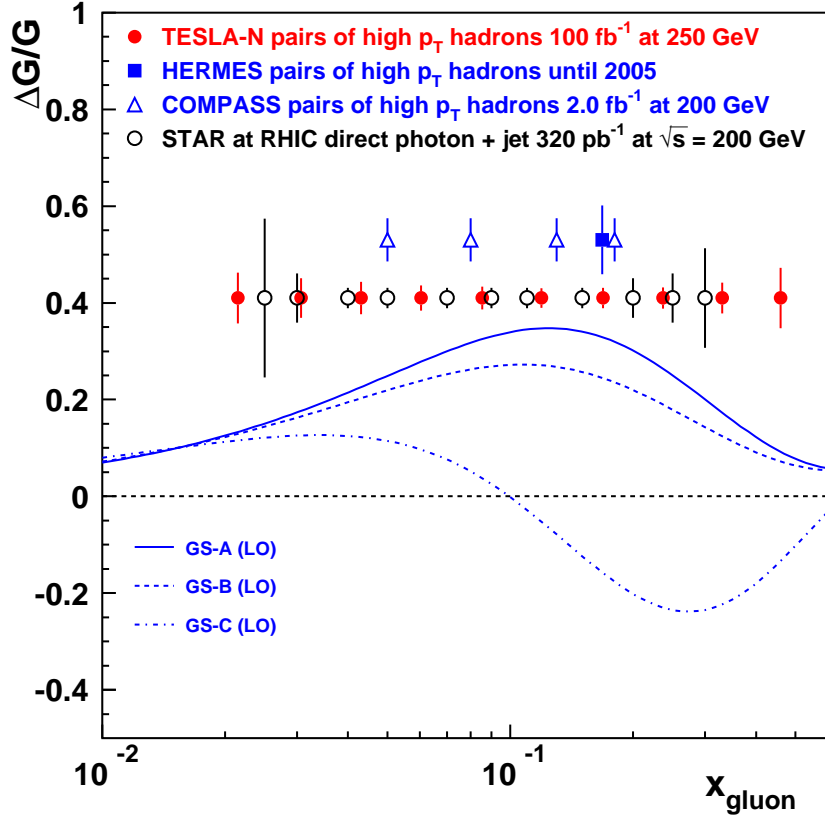


Fig. 5. Projected statistical accuracies for the measurement of $\Delta G(x)/G(x)$, based on an integrated luminosity of 100 fb^{-1} , in comparison to projections from RHIC [34], HERMES [35], and COMPASS [36]. A study of the systematic uncertainties due to the x_{gluon} reconstruction procedure and due to QCDC background (right-most points) has not yet been completed. The phenomenological predictions [37] were calculated for $Q^2 = 10 \text{ GeV}^2$.

The projected TESLA-N accuracy to measure $\Delta G(x)/G(x)$ is shown in figure 5, in comparison to projected accuracies for HERMES, COMPASS and RHIC. In comparison to COMPASS, TESLA-N will have at least 50 times more statistics (cf. section 3.4). Hence it will be the only envisaged polarized lepton-nucleon scattering experiment capable to determine the ratio $\Delta G(x)/G(x)$ over a wide range of x with an impressive statistical accuracy; systematic uncertainties have still to be studied (cf. caption). The overall x -range and the projected precision of the STAR measurement at RHIC are comparable to the TESLA-N projection. For completeness it has to be mentioned that high accuracy at large x can also be realized at JLAB, but their ‘theoretical’ systematic error can hardly be reduced below that at HERMES because of their low center-of-mass energy.

In addition to the direct methods described above, QCD NLO fits to the spin structure function $g_1(x, Q^2)$ are able to yield a parametric form of $\Delta G(x, Q^2)$. However, no QCD fit to the existing data has yet been able to deliver a statistically convincing determination of

even the first moment $\Delta G(Q^2) = \int_0^1 dx \Delta G(x, Q^2)$. At present, this *indirect* determination of $\Delta G(x, Q^2)$ is problematic, because at lower energies the effects of the evolution due to $\Delta G(x, Q^2)$ cannot be cleanly separated from higher-twist effects. A precision measurement of $g_1(x, Q^2)$ at TESLA-N will dramatically enlarge the accuracy and the kinematic range, as can be concluded from figure 4. To obtain a projection for the first moment, a QCD NLO fit was performed in the $\overline{\text{MS}}$ scheme using all DIS data published until summer 2000, giving a result of 0.43 ± 0.21 (stat.), at the scale of $Q^2 = 1 \text{ GeV}^2$. The resulting structure function $g_1(x, Q^2)$, in its parametric form, was then evolved into the kinematical region of TESLA-N and then used as additional input data for two new fits. Adding data that correspond to 100 fb^{-1} using a proton target improves the statistical accuracy down to ± 0.06 . An additional data set obtained with 100 fb^{-1} on a deuteron target yields a further improvement down to ± 0.04 . This additional deuteron data set considerably improves the statistical accuracy in the determination of the non-singlet quark distribution in the neutron, when comparing to existing data.

A comparison of this indirect determination of $\Delta G(x, Q^2)$ with the above described direct determinations will allow important consistency checks that in the end will lead to a reliable picture of how the gluons contribute to the nucleon spin.

Last, but not least, results for the *unpolarized* gluon distribution at large x are of great importance to many searches for new physics and to the uncertainties in estimating conventional cross sections in the large- x region for background processes to the Higgs-search at LHC. Present fits to the unpolarized gluon distribution in the region $x > 0.15$ are still dominated by the old and partially inconsistent data of NA14/2, E691 and E687. The most suitable processes to determine the unpolarized gluon distribution at large x are, as in the polarized case, heavy-quark pair production and the production of pairs of high- p_\perp hadrons. These measurements will automatically also be available at TESLA-N.

2.4 Higher Twist

TESLA-N will be able to address a central issue of the present-day QCD discussions in inclusive and semi-inclusive physics, namely the role of higher twist. It is clear that the applicability of perturbative QCD will eventually come to an end for low photon virtualities due to the increase of higher-twist effects. They hence play a crucial role in relating conventional perturbative QCD results to the bulk of hadron phenomenology. Today it is difficult to predict at which scales higher-twist contributions become important in the small- x and large- x domain of the different observables since the relevant parameters controlling them are non-perturbative. Currently this is not even known for the well measured unpolarized structure function $F_2(x, Q^2)$. In addition, higher-order QCD corrections and higher-twist corrections cannot be dealt with independently (cf. e.g. [38–41]). The knowledge of these corrections is also important for the presently available polarized data, which lie mostly in the Q^2 -domain of only a few GeV^2 . Obviously, a higher-twist analysis based on high precision data for $g_1(x, Q^2)$ could help to clarify the situation substantially. This would also be important for spin physics in general, because it would reduce in present-day fits the uncertainties due to neglected higher-twist contributions.

A precise measurement of the spin structure function $g_2(x, Q^2)$ remains a major challenge for future polarized DIS experiments with transverse target polarization. The measure-

ments obtained so far [42] will be improved by TESLA-N, extending the measurements down to x -values of $5 \cdot 10^{-3}$. Besides its twist-2 contribution $g_2(x, Q^2)$ contains a twist-3 term the isolation of which is important. At lowest order in QCD twist-2 and twist-3 contributions to $g_1(x, Q^2)$ and $g_2(x, Q^2)$ are connected by integral relations [43–46] which can be tested in this way. Moreover, if the Q^2 -dependence of the twist-3 contribution to $g_2(x, Q^2)$ can be isolated the validity of new QCD evolution equations, cf. e.g. [47], can be tested. Both issues provide new and important tests of QCD.

There are several more distribution and fragmentation functions for polarized electron-nucleon scattering. Mulders and collaborators have given a classification of all twist-2 and twist-3 functions [11,12]. From a purist’s point of view it can be argued that all of them are equally important, as they all test different features of nucleon structure and fragmentation dynamics. A more phenomenological point of view would be to concentrate on those that have an intuitive physics significance or probe specific QCD dynamics. Presently a lot of theoretical work is invested into the development of such an intuition (cf. e.g. [48]).

2.5 Fragmentation Functions

A comprehensive study of fragmentation processes is of great value in itself. To make full use of the data collected by the B-factories and (partly) LHC will require a good understanding of many different fragmentation processes. The high quality DIS data generated by TESLA-N would allow the fine-tuning of the fragmentation codes used for this purpose. Contemporary semi-inclusive analyses usually assume knowledge of the fragmentation functions, as obtained from $e^+e^- \rightarrow hX$, and use these as a tool in studying the parton distribution functions. However, several new analyses of the e^+e^- data have appeared [51–53]. All agree very well with the data, yet their derived fragmentation functions differ significantly; in some regions of z by 40-100 %. As a result, it has become crucial to use semi-inclusive DIS data to measure parton distributions as well as fragmentation functions. There is no problem of principle; all that is required is a sufficiently large amount of high quality data [54]. While this is beyond present day experiments, TESLA-N should be able to stand up to the challenge. However, no specific projections have been worked out yet.

2.6 Specific Deuteron Structure Functions

In deep-inelastic scattering on a polarized spin 1 target new structure functions are involved that do not appear for a spin $\frac{1}{2}$ target. At leading twist the new functions are $b_{1(2)}(x, Q^2)$ [49] and $\Delta(x, Q^2)$ [50]. These hitherto completely unknown structure functions measure the extent to which the deuteron is not a trivial bound state of proton and neutron. $\Delta(x, Q^2)$ is especially interesting since it describes a flip of the photon helicity by two units. It probes the gluonic components of the deuteron wave function which cannot be identified with any contribution from the constituent nucleons or virtual pions.

The structure functions $b_{1(2)}(x)$ are accessible when the polarized electron beam is scattered off longitudinally polarized deuterons. The measurement of $\Delta(x, Q^2)$ requires an unpolarized electron beam and transversely polarized deuterons. In the latter case a characteristic azimuthal angular dependence of the cross section, $d\sigma \sim \cos 2\phi$, is predicted.

All these specific deuteron structure functions are expected to be of rather small size and thus a high luminosity polarized experiment as TESLA-N appears to be the ideal place to access information on this non-trivial parton composition of the deuteron.

3 Layout of the Experiment

3.1 Polarized Target

One of the main ingredients of the TESLA-N apparatus is the polarized target. To reach the required high luminosity with a small fraction (20 nA, cf. section 3.2) of the total TESLA current (45 μ A) a polarized solid state target of about 1 g/cm² areal density was chosen, similar in design to the one used at SLAC [55].

The polarized target will consist of a ⁴He evaporator cryostat, a 5 T Helmholtz-type magnet and a 140 GHz microwave system for permanent Dynamic Nuclear Polarization. The polarization is measured by Nuclear Magnetic Resonance. The maximum allowed heat load on the target is limited by the cooling power of the evaporator cryostat to about 1 W at a temperature of 1 K. The total heat load on the target due to the beam for a current of 20 nA has been calculated to be only about 50 mW [56]. Hence, there should be no basic problem with the cooling. Because 1 K is rather warm on the temperature scale of polarized targets, a strong magnetic field must be chosen to achieve reasonably high polarization values. The magnetic field is limited to 5 T, because the power of microwave sources with frequencies higher than 140 GHz is insufficient today. A symmetric Helmholtz design of the magnet combines excellent homogeneity with large opening angles for both, longitudinal and transverse polarization. The two main criteria for the choice of the target material are low dilution by unpolarized nucleons and resistance against radiation damage with respect to the intense TESLA beam. Therefore NH₃ ($P_T = 0.8$, $f = 0.176$) and ⁶LiD ($P_T = 0.3$, $f = 0.44$) presently appear as the best choices to study electron scattering off polarized protons or deuterons.

A large number of physics questions can be addressed in high luminosity running with different *unpolarized* nuclear targets. Targets with very high atomic numbers can be easily constructed forming appropriately thin foils. In this case electron beam currents may be possible that are considerably higher than 20 nA.

3.2 Polarized Electron Beam

The electrons for TESLA-N will be accelerated together with the positrons in the north arm of the TESLA main accelerator. This ‘opposite charge option’ was chosen to be able to realize a separation between the beam for the eN-experiment and the main beam by a static magnet system. This system would have a length of about 150 m and be located upstream of the separation for the two main interaction points (cf. figure 10). The beam energy initially will be 250 GeV; energies up to 500 GeV may be possible in a later phase of TESLA.

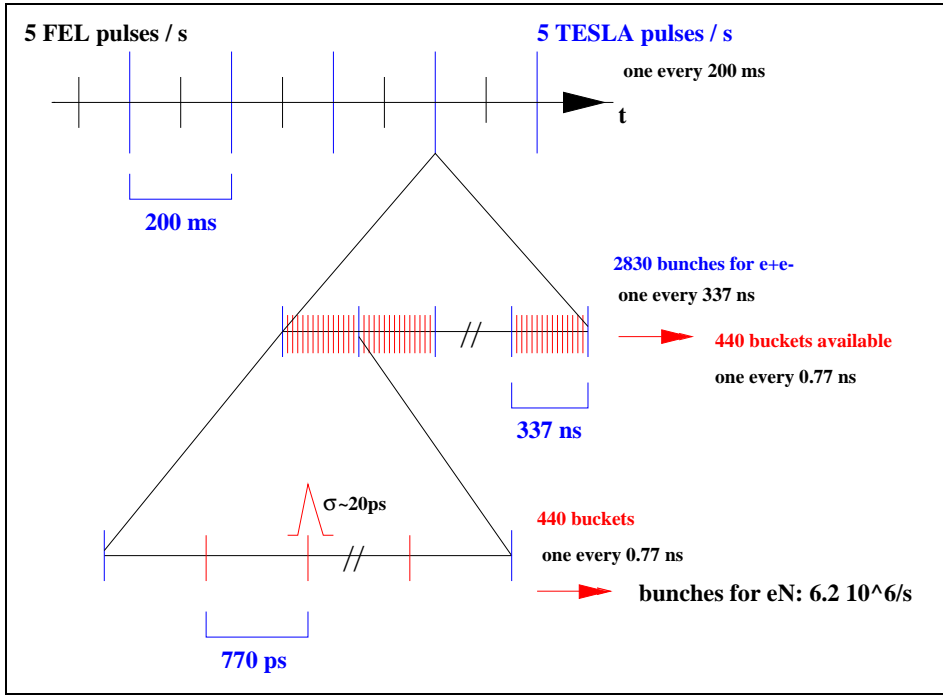


Fig. 6. Time structure of the polarized electron beam in TESLA (south arm) fully exploiting the 1.3 GHz machine frequency.

Both TESLA arms are planned to run with a 5 Hz macropulse repetition rate for e^+e^- -operation. Additional 5 Hz will be run along a limited fraction of the south arm to facilitate FEL operation. The corresponding time structure of the polarized electron beam is illustrated in figure 6. The 0.5 % north arm duty cycle in conjunction with the basic machine frequency of 1.3 GHz has most severe consequences for the proposed experiment. Using the same time structure as foreseen for the e^+e^- -experiment, i.e. one bunch of 20 ps length crossing the target every 337 ns, would result in as much as a few hundred quasi-real photo-production events within these 20 ps. This is an unacceptably high rate for an eN-experiment, because the scattered electron must be uniquely assigned to the hadrons produced in the same interaction. To minimize the number of multiple events per beam crossing while maximizing the luminosity, it is foreseen to fill every bucket of the bunch train (one every 0.77 ns), while limiting the beam current to 20 nA. This corresponds to 20k electrons per bunch and to 6.2 million bunches per second crossing the TESLA-N target.

Although being beyond the scope of the present study, it should be noted that a few improvements for eN-operation appear to be feasible.

- (1) Also along (part of) the north arm a 10 Hz macropulse repetition rate could be used. This would double all performance figures for e^-N -operation.
- (2) Two intermediate ejection points are technically feasible. For the FEL, i.e. in the south arm, there will be 2 ejection points (at about 25 and 50 GeV). By RF tuning a dynamic range of about 2 will be routinely available, such that de facto energies 12.5 to 25 GeV (at point 1) and 25 to 50 GeV (at point 2) can be 'dialed'. It is technically feasible to have two ejection points also in the north arm at e.g. 50 and 100 GeV. This would allow the selection of any energy between 25 and 100 GeV in addition to the full energy of 250 GeV.

Physics requirements suggest to study e^+N -interactions as well. It is technically unprob-

lematic to install an additional (low intensity) positron source besides the separate electron source that is already required for e^-N operation. Since the 'eN-positrons' will need a kicker magnet to be separated from the 'collider-positrons', only the extra 5 macro pulses in the 10 Hz 'a la FEL' mode could be used, thus limiting the duty cycle to 0.5%. Presently no solution is known to obtain polarized positrons in such a configuration. The production of polarized positrons requires > 150 GeV electrons, as planned for TESLA e^+e^- operation. However, at present it appears not realistic to assume that this system could also deliver polarized positrons for eN.

An electron current of 20 nA constitutes only about 0.04% of the main beam current. Therefore the energy consumption for beam acceleration at TESLA-N can be considered to be almost negligible. This advantage implies the drawback that monitoring of the small electron beam cannot be done together with that of the high current beam in the main linac, but only before and after acceleration. This requires further studies.

3.3 Overview of the Apparatus

In a fixed-target electron-nucleon scattering experiment at 250 GeV, acceptable resolutions in particle momentum and scattering angle may only be achieved by using a multi-stage spectrometer. A schematic sketch of a possible TESLA-N apparatus is shown in figure 7. All three stages of the spectrometer will use large dipole magnets (SM1-3) for momentum analysis. As can be seen from the figure, the overall dimensions of the TESLA-N apparatus are comparable to those of COMPASS [3] because the kinematics of both experiments are similar.

Most hadrons are to be measured in Stage 1, while most of the scattered electrons and, in addition, a part of the leading hadrons will be detected in Stage 2. For both Stage 1 and 2 electron/hadron separation, hadron identification, and electron/photon separation will be very important and hence their design looks similar to the HERMES spectrometer [57]. Stage 3 is required to detect scattered electrons down to the lowest possible angles and will need adequate tracking capabilities combined with some electron/hadron separation.

While at COMPASS a thick target is traversed by incoming muons, the relatively thin solid state target planned for TESLA-N will be hit by electrons that cause a much higher rate of bremsstrahlung. Its rate amounts to about 20% of the incoming electron rate at a target thickness of 1 g/cm^3 . Due to the magnetic deflection, the resulting lower momentum electrons form a 'sheet of flame' on their way down the spectrometer. While the width of the sheet-of-flame itself is below 1 mm, its effective width corresponds to a possible wobbling area of the incoming electron beam that must be of the order of a few mm to match the target size. The electrons and the bremsstrahlung photons must not meet any material in their way to avoid background showers. The safest way to ensure this is to provide a vacuum chamber that contains not only the high energy beam electrons, but also the sheet-of-flame electrons and the radiated photons, as well as the synchrotron radiation produced in the three spectrometer magnets and the target magnet. Instead of only a vacuum pipe an extended vacuum vessel appears to be necessary. This vessel forms a narrow 'slit' whose height (in the bending plane) is increasing along the spectrometer, while its width can be as low as ± 2 cm.

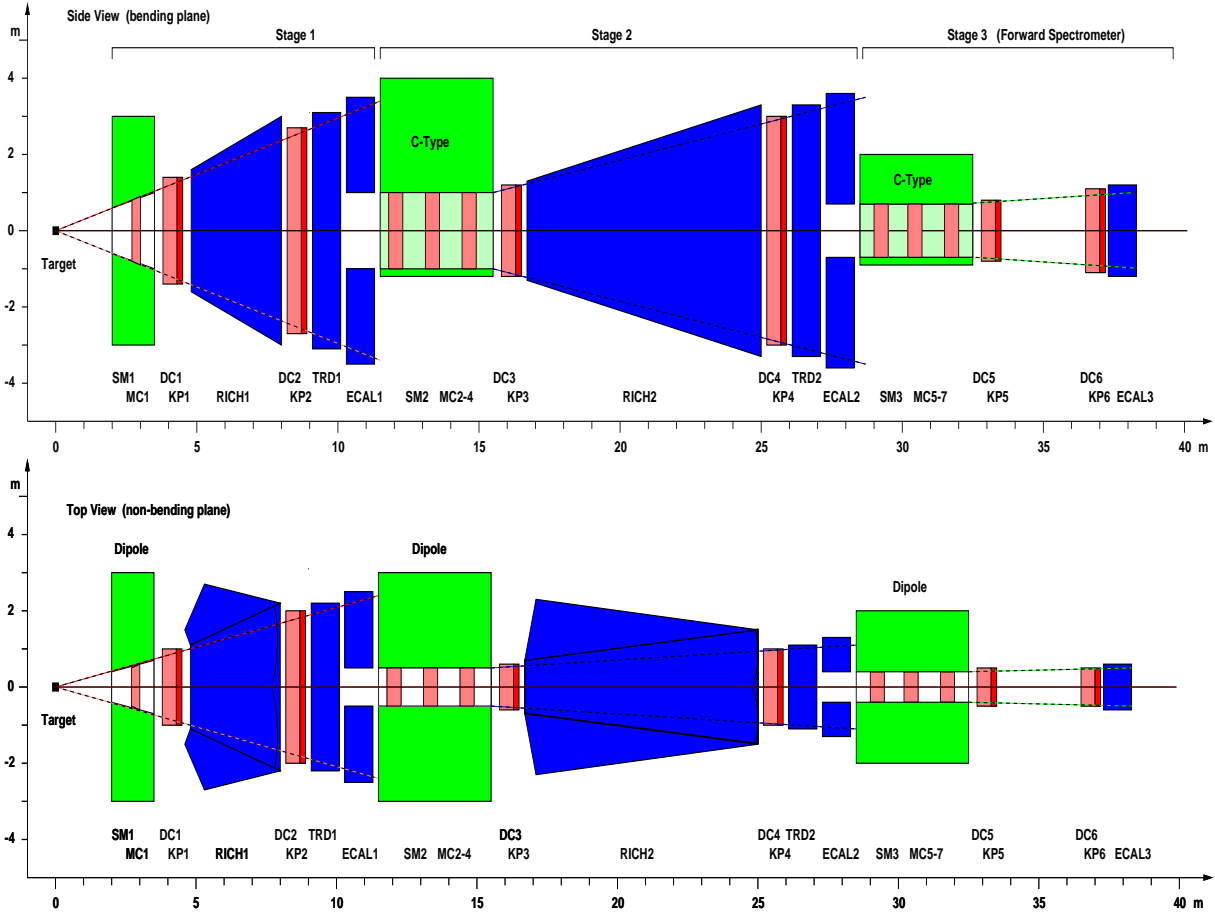


Fig. 7. Schematic side view and top view of the envisaged TESLA-N apparatus. For an explanation of the acronyms see the text.

The sheet-of-flame must be oriented towards a beam dump close to the experiment. To this end, the dipole fields in SM1-3 should be oriented horizontally and the above mentioned vacuum vessel extends vertically down from the beamline. As a further consequence, SM2 and SM3 will most likely be C-type magnets. The integrated magnetic fields will be 2 Tm for SM1 and 5 Tm each for SM2 and SM3.

The envisaged very high luminosity of the experiment leads to very high interaction rates, so that a few hundred charged tracks can be expected per ‘recorded event’. Here ‘recorded event’ stands for the pile-up of physics events over the typical integration time of the tracking detectors (cf. section 3.4). These conditions make it impossible for a single tracking device to have both the required very fast response and the necessary position resolution. Therefore it is planned to combine fast tracking detectors (e.g. scintillating fibres), so-called ‘key planes’ (KP1-6), with precise tracking detectors. These detectors could be drift chambers (DC1-6). Similar to COMPASS, where a 2 ns resolution was shown recently [58], the fast but less precise detectors will serve to ‘snapshot’ events on the bunch level which cannot be resolved by the slow but precise detectors (‘fast-slow tracking’).

The first section of SM1 will bend out the particles with momenta below a few hundred MeV. Hence a first slow and less precise position detector (‘magnet chamber’, ‘MC1’) may possibly be already accommodated within the gap of SM1. Since Stage 1 of the spectrometer will analyse predominantly particles in the momentum range of 1 to some 10 GeV, where multiple scattering is still an issue, the thickness of all Stage 1 tracking

detectors must be optimized against their precision and possibly a large low pressure container will be used. Choosing 150 ns as a representative integration time for the ‘slow’ detector, the cell size of all detectors must be small enough to deal with the expected high occupancies. The requirements for the Stage 2 detectors are expected to be less severe.

The electron-hadron separation in both Stage 1 and 2 will be provided by combinations of transition radiation detectors with electromagnetic calorimeters (TRD1/2, ECAL1/2), complemented by ring-imaging Cerenkov detectors for hadron identification (RICH1/2). For Stage 3 only an electromagnetic calorimeter (ECAL3) is foreseen. In addition, the gaps of SM2 and SM3 can be instrumented with suitable tracking detectors, e.g. proportional chambers (MC2-7), to minimize acceptance losses. Both ECAL1 and ECAL2 must not cover the entrance cone to the next spectrometer stage, while all other detectors in Stage 1 and 2 have to be designed with the central slit for the through-going flux of photons and high energy electrons, as discussed above.

Certain reaction channels greatly benefit from additional kinematic constraints that can be obtained by measuring ‘recoil’ particles. In the given kinematics, recoil particles leave the target under laboratory polar angles of a few tens of degrees. Their detection can hence be accomplished by a small-size barrel detector [56] surrounding the target and/or forward ‘wheels’ similar to those developed at HERMES [59]. The target holding field may even allow for some momentum analysis, while some particle identification may be possible through ionization signals.

3.4 *Luminosity and Acceptance*

An areal target density of 1 g/cm² of polarizable material that is hit by bunches carrying 20k electrons each, leads to a maximum possible luminosity of 12 mb⁻¹ per bunch. With the above explained 6.2 million bunches per second this corresponds to a luminosity of $7.5 \cdot 10^{34}$ cm⁻² s⁻¹, which represents the maximum value possible with the present TESLA design.

Table 1 shows the envisaged luminosity of TESLA-N in comparison to other current or planned electron scattering facilities. The first entry corresponds to the present TESLA design with a 5 Hz macropulse repetition rate in the north arm; the second entry applies if a (technically feasible) rate of 10 Hz is assumed (cf. section 3.2). When comparing luminosities of fixed-target experiments (upper panel) and collider experiments (lower panel), the degree of polarization and purity (= fraction of the polarized material) of the involved nucleon have to be taken into account. For example, when comparing a polarized NH₃-target and a circulating proton beam, the effective luminosity of the polarized fixed-target experiment is lower by a factor of about 25.

Adopting a conservative ansatz for efficiencies, namely a combined up-time of accelerator and experiment of 0.33 in conjunction with an efficiency of the experiment of 0.75, results in the conservative overall efficiency factor of 0.25. This factor leads to maximum achievable integrated luminosities for TESLA-N of 1.6 fb⁻¹ per effective day, 50 fb⁻¹ per effective months, and 600 fb⁻¹ per effective year. The term ‘effective’ was chosen here to characterize a running period during which both accelerator and experiment operate routinely including all usually occurring day-by-day problems.

Experiment	c.m. Energy [GeV]	Luminosity [$\text{cm}^{-2} \text{s}^{-1}$]
TESLA-N	22	$7.5 \cdot 10^{34}$
TESLA-N (10 Hz)	22	$1.5 \cdot 10^{35}$
COMPASS	20	$5.0 \cdot 10^{32}$
SLAC (incl.)	$5 \div 10$	$5.0 \cdot 10^{34}$
HERMES (unpol.)	7.2	$4.0 \cdot 10^{33}$
HERMES (pol.)	7.2	$2.0 \cdot 10^{31}$
ELFE@CERN (unpol.)	7	$1.0 \cdot 10^{38}$
ELFE@CERN (pol.)	7	$5.0 \cdot 10^{35}$
HERA $\vec{e}\vec{p}$	318	$1.0 \cdot 10^{31}$
HERA eA	150	$1.0 \cdot 10^{30}$
eRHIC	100	$2.0 \cdot 10^{32}$
EPIC	31	$1.0 \cdot 10^{33}$

Table 1

Comparison of luminosities and c.m. energies for current and planned electron scattering facilities

At maximum luminosity every bunch (one every 0.77 ns) produces on average 0.2 quasi-real-photonproduction events with $\nu > 3$ GeV. For an average multiplicity of about 3 detected charged hadron tracks per physics event this corresponds to about 100 hadron tracks in Stage 1 per recorded event. The typical integration time and thus the length of the recorded event is assumed to be 150 ns, corresponding to about 200 bunches. The additional rate from Möller electrons with an energy above 1.5 GeV amounts to about 1 per bunch, or about 200 electron tracks per recorded event. However, Möller electrons reaching the spectrometer can be uniquely distinguished from DIS electrons with $Q^2 > 1$ GeV² by their kinematics. Only about one DIS event with $Q^2 > 1$ GeV², $W^2 > 4$ GeV² and polar angles above 5 mrad will be contained in one recorded event.

A crucial question for the analysis of DIS events is whether they can be cleanly identified or whether they are mixed with other events. For the above quoted 0.2 photoproduction events per bunch about 18% of all DIS events will be accompanied by a photoproduction event produced by the same bunch. Off-line cuts on the total deposited energy, the track multiplicity and the energy of the leading hadron have to be used to identify and remove these events. From preliminary considerations it is expected that in the end this multiple event fraction for DIS events can be safely reduced to a level of about 1% or less.

In certain areas more work has to be invested to solidify the assumptions made above:

- i) It is presently assumed that a time resolution of 0.77 ns can be realized in the future for the fast tracking detectors at TESLA-N. As it was proven recently, today's technology already allows to reach 2 ns [58]. In a conservative approach a beam current lower by a factor of 3 would have to be assumed.
- ii) The method to reduce the multiple event fraction in a DIS event from 18% to the envisaged 1% can only be developed on the basis of a careful Monte Carlo study. There is very little doubt that a factor of 3 can be realized easily. In a conservative approach a beam current lower by a factor of 6 would have to be assumed to arrive at the design value of 1%.

It is anticipated that adequate answers can be found for these questions. To leave a ‘safety margin’ until the above questions will have been answered, it was decided to assume for all physics projections a reduction of the beam current, i.e. consequently also of the luminosity, by a factor of 6. This decrease in beam current will relieve both point i) and ii). In the most conservative approach, where both i) and ii) are taken at their lower limits, the beam current and thus the luminosity for the physics projections needs not to be reduced further than the factor of 6, because another factor of 3 can be gained by running for three years instead of one. Altogether it thus appears to be a well-founded starting point that 100 fb^{-1} per effective year is the conservative integrated luminosity of TESLA-N. This number was taken to calculate all projected statistical uncertainties throughout this document. It appears worth noting that it is still a factor of 50 above the maximum achievable integrated luminosity of 2 fb^{-1} , presently planned for one effective year of COMPASS running with the same overall efficiency factor of 0.25.

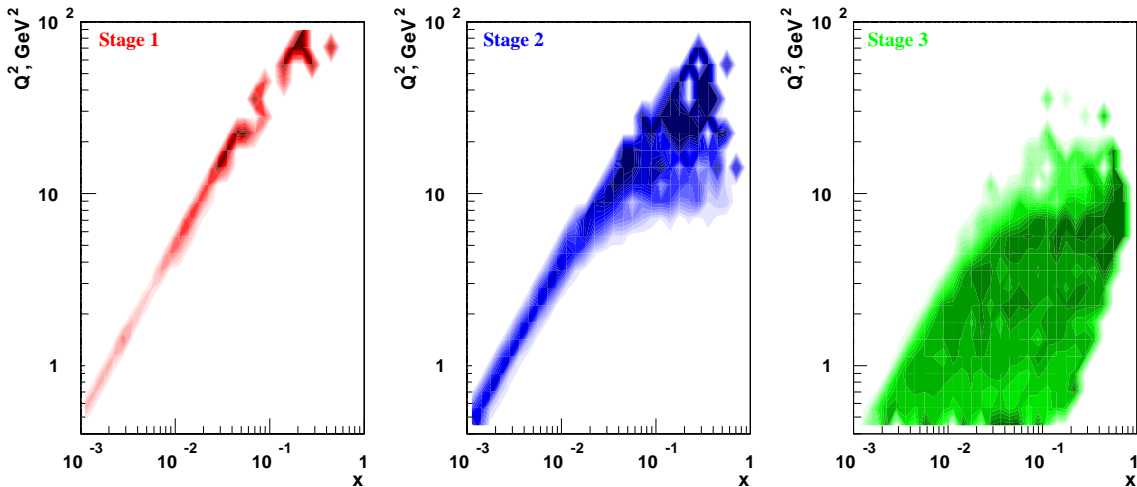


Fig. 8. Acceptance of the TESLA-N spectrometer for the scattered electron.

The acceptance of the TESLA-N spectrometer for the scattered electron in the (x, Q^2) plane is shown in figure 8. Electrons with high Q^2 ($>10 \text{ GeV}^2$) are predominantly detected in Stage 2, while low- Q^2 electrons ($<10 \text{ GeV}^2$) are detected in Stage 3. Figure 9 shows the acceptance for leading hadrons as a function of $z = E_h/\nu$. More than 80% of all leading hadrons are detected in Stage 1 of the spectrometer while about 40% of them are detected both in Stage 1 and 2 (for $z > 0.15$). As a result, these hadrons are detected with good momentum resolution independently of the vertex reconstruction. The opening of SM1 limits the acceptance to $\theta_x \leq 225 \text{ mrad}$ and $\theta_y \leq 280$. The lowest possible detection angle θ_{min} is about 5 mrad for momentum analysis within Stage 2 including the detection plane in front of SM 2. If Stage 3 is used including the detection plane in front of SM 3, θ_{min} can be reduced to values as low as 2-3 mrad. These approximate figures are based on a width of the vacuum vessel of $\pm 2 \text{ cm}$ and a width of the DC frame next to it of 3 cm. For electrons, θ_{min} directly determines the lowest reachable Bjorken- x .

3.5 Resolution in Kinematic Variables

Reliable values for the individual detector resolutions are not yet worked out. A momentum resolution on the level of 0.5 % appears to be a reasonable assumption. It can be achieved in spectrometer Stage 2 for tracks with momenta below 100 GeV, if a (realistic)

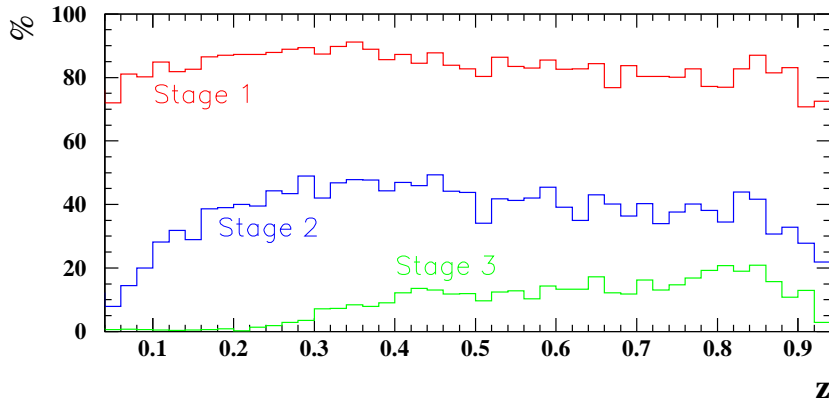


Fig. 9. Acceptance of the TESLA-N spectrometer for the leading hadron.

position resolution of about $100 \mu\text{m}$ per space point is available. A similar momentum resolution for tracks crossing Stage 3 with momenta up to 200 GeV requires better position resolutions. For the angular resolution 0.3 mrad can be assumed as a preliminary value. The expected spread in the beam momentum (0.1%) is small enough to not affect the resolution in any of the kinematic variables. Possible beam energy losses prior to the interaction have not been studied yet.

The resolutions in the different kinematic variables are characterized by two different effects. On the one hand, the resolution in Q^2 is dominated by the resolution in the electron scattering angle. Only an angular resolution of the order of 0.3 mrad or better can lead to Q^2 -resolutions at the level of a few % at large x -values. None of the other spectrometer resolutions have such a strong impact on the Q^2 resolution. On the other hand, the resolution in the variables ν , x and z is dominated by the momentum resolution of the spectrometer that, in turn, has little impact onto the Q^2 resolution.

Most of the non-leading and part of the leading hadrons will be detected in the Stage 1 of the spectrometer while the higher-momentum leading hadrons will be measured both in Stage 1 and Stage 2. A moderate *hadron* momentum resolution of the order of 1% would be acceptable, provided that the electron momentum resolution is good enough.

3.6 Civil Engineering

The basic layout for the proposed eN-experiment within the mostly fixed TESLA infrastructure is shown in figure 10.

A separate electron gun system is required for TESLA-N at the north end of the TESLA machine. It is envisaged to use a laser driven strained GaAs SLAC-type gun that must be made capable to deliver 20k highly polarized electrons per 0.77 ns. It must be followed by a separate preaccelerator whose end energy and type are under discussion. Present options are a TESLA-type accelerator or a normal-conducting MAMI-type microtron. A short extra tunnel is required from the separation building to the TESLA-N hall. The TESLA-N experimental hall would be placed as far north as the site permits to minimize construction costs. An extra beam absorber is required.

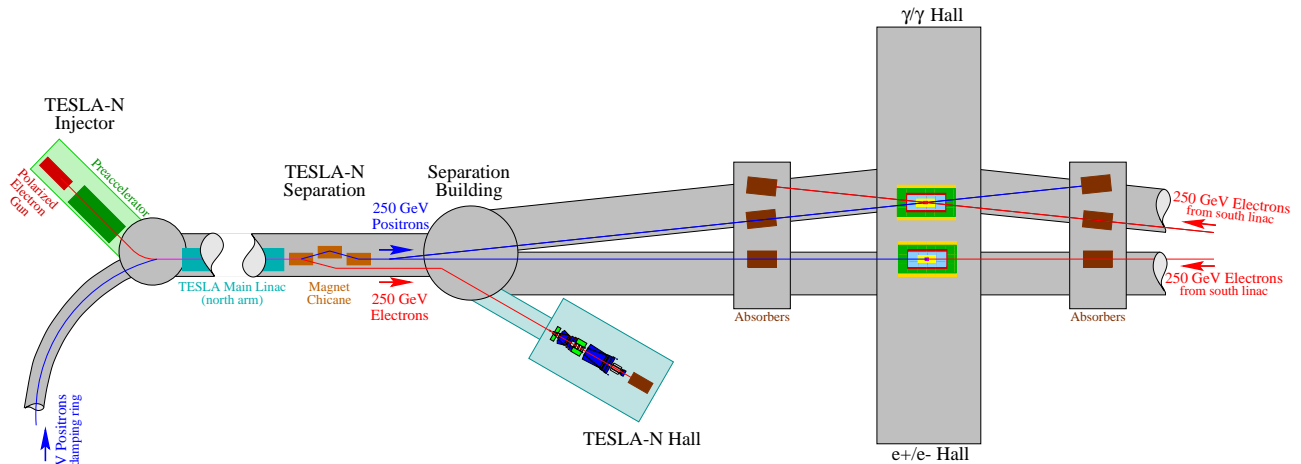


Fig. 10. Schematic top view of the machine-related elements.

4 Summary

This document presents the prospects for a polarized deep-inelastic electron-nucleon scattering experiment at the TESLA facility at DESY. For the first time a complete mapping of the Q^2 - and x -dependence of both the helicity and the transversity distributions Δq and δq will become possible. Complemented by precise results on the polarized gluon distribution most of the components of the angular momentum structure of the nucleon will be determined with high precision. Hence, the measurements foreseen at TESLA-N will constitute one of the most comprehensive and precise investigations of hadronic properties and tests of QCD techniques in the polarized sector. These measurements will open an access to the hitherto unknown chirally odd operators in QCD and thus greatly improve the understanding of the role of chiral symmetry.

A possible layout for a fixed-target electron-nucleon scattering experiment TESLA-N is presented as well. A separate hall is foreseen north of the main e^+e^- -interaction point. First design considerations for a polarized target, a three-stage spectrometer and a recoil detector are discussed. It is concluded that the experiment is technically feasible, although many aspects of the design require further study.

The proposed deep-inelastic eN-experiment at TESLA constitutes a highly competitive and very cost-effective solution. It will be unique as it combines high luminosity with large center-of-mass energies, using highly polarized electron beams and targets. The possibilities of using unpolarized targets and of experiments with a real photon beam turn TESLA-N into a versatile next-generation facility at the intersection of particle and nuclear physics. Finally, this experiment would be the natural continuation of the HERA tradition at DESY in studying the structure of the nucleon with electromagnetic probes.

References

- [1] O. Martin, A. Schäfer, M. Stratmann, W. Vogelsang, *Phys.Rev.* **D60**, 117502 (1999)
- [2] HERMES Collaboration, Hermes internal note 00-003, DESY, 2000.
- [3] COMPASS Collaboration, CERN/SPSLC 96-14 (1996).
- [4] R. L. Jaffe, MIT-CTP-2685, hep-ph/9710465.
- [5] P. V. Pobylitsa et al., Bochum University preprint RUB-TPII-15/00
- [6] S. Aoki, M. Doui, T. Hatsuda and Y. Kuramashi, *Phys. Rev.* **D56**, 433 (1997)
- [7] S. Capitani et al., DESY 99-064, 1999
- [8] J.C. Collins, *Nucl. Phys.* **B396**, 161 (1993)
- [9] J.C. Collins, S.F. Heppelmann, G.A. Ladinsky, *Nucl. Phys.* **B420**, 565 (1994)
- [10] A.M. Kotzinian, P.J. Mulders, *Phys. Lett.* **B406**, 373 (1997).
- [11] P.J. Mulders, R.D. Tangermann, *Nucl. Phys.* **B461**, 197 (1996)
- [12] D. Boer and P.J. Mulders, *Phys. Rev.* **D57**, 5780 (1998)
- [13] J. C. Collins and G. A. Ladinsky, hep-ph/9411444
- [14] R. L. Jaffe, X. Jin and J. Tang, *Phys. Rev. Lett.* **80** (1998) 1166
- [15] A. Bianconi, S. Boffi, R. Jakob and M. Radici, *Phys. Rev.* **D62** 034008 (2000)
- [16] V. Barone, *Nucl.Phys.* **A666-667**, 282 (2000)
- [17] X. Ji, *Phys. Rev.* **D 49**, 114 (1994)
- [18] A. Bacchetta, P.J. Mulders, VUTH 00-20, hep-ph/0007120
- [19] V.A. Korotkov, W.-D. Nowak, K.A. Oganessyan, DESY 99-176, hep-ph/0002268.
- [20] M. Glück et al., *Phys. Rev.* **D53**, 4775 (1996)
- [21] J. Soffer, *Phys. Rev. Lett.* **74**, 1292 (1995)
- [22] O. Martin, A. Schäfer, M. Stratmann, W. Vogelsang, *Phys.Rev.* **D57**, 3084 (1998)
- [23] A. Schäfer and O. Teryaev, *Phys.Rev.* **D61**, 077903 (2000)
- [24] HERMES Coll., A. Airapetian et al., *Phys. Rev. Lett.* **84**, 9047 (2000)
- [25] A.V. Efremov, O.G. Smirnova, L.G. Tkachev, *Nucl. Phys. Proc. Suppl.* **74**, 49 (1999)
- [26] G. Ingelman, A. Edin, J. Rathsman, *CPC* **101**, 108 (1997)
- [27] T. Sjöstrand, *CPC* **82**, 74 (1994)
- [28] B. Adeva et al., *Phys. Lett.* **B420**, 180 (1998)
- [29] HERMES Coll., K. Ackerstaff et al., *Phys. Lett.* **B464**, 123 (1999)
- [30] K. Goeke, P.V. Pobylitsa, M.V. Polyakov, D. Urbano, hep-ph/0003324
- [31] A. Bravar, D. v.Harrach, A. Kotzinian, *Phys. Lett.* **B421**, 349 (1998)

- [32] M. Glück, E. Reya, W. Vogelsang, *Nucl. Phys.* **B351**, 579 (1991)
- [33] HERMES Coll., A. Airapetian et al., *Phys. Rev. Lett.* **84**, 2584 (2000)
- [34] L. Bland, hep-ex/9907058
- [35] E. Aschenauer, W.D. Nowak, private communication
- [36] J. Nassalski, *Acta Phys. Pol.* **B29**, 1315 (1998)
- [37] T. Gehrmann, W.J. Stirling, *Phys. Rev.* **D53**, 6100 (1996)
- [38] U.K. Yang and A. Bodek, *Eur. Phys. J.* **C13**, 241 (2000)
- [39] A.L. Kataev et al., *Phys. Lett.* **B417**, 374 (1998)
- [40] A.L. Kataev, G. Parente, A.V. Sidorov, hep-ph/0001096
- [41] E. Stein, M. Maul, L. Mankiewicz, A. Schäfer, *Nucl. Phys.* **B536**, 318 (1998)
- [42] E155x Coll., P. Bosted et al., *Nucl. Phys.* **A663–664** (2000) 297.
- [43] S. Wandzura and F. Wilczek, *Phys. Lett.* **B72** (1977) 195.
- [44] A.V. Efremov, E. Leader, O.V. Teryaev, *Phys. Rev.* **D55** (1997) 4307
- [45] J. Blümlein, A. Tkabladze, *Nucl. Phys.* **B553** (1999) 427
- [46] J. Blümlein, A. Tkabladze, *Nucl. Phys. B Proc. Suppl.* **79** (1999) 541.
- [47] V.M. Braun, G.P. Korchemsky, and A.N. Manashov, *Phys. Lett.* **B476** (2000) 455.
- [48] M. Anselmino, F. Murgia, DFTT-06-2000, hep-ph/0002120
- [49] R.L. Jaffe, A. Manohar, *Nucl. Phys.* **B321**, 343 (1989)
- [50] R.L. Jaffe, A. Manohar, *Phys. Lett.* **B223**, 218 (1989)
- [51] S. Kretzer, *Phys. Rev.* **D62**, 054001 (2000)
- [52] B.A. Kniehl, G. Kramer, B. Pötter, hep-ph/0003297
- [53] L. Bourhis et. al., hep-ph/0009101
- [54] E. Christova, E. Leader, hep-ph/0007303
- [55] K. Abe et al., *Phys. Rev.* **D58**, 112003(1998)
- [56] J.J.M. Steijger, G. v.d. Steenhoven, NIKHEF 2000-013
- [57] K. Ackerstaff et al., *NIM* **A417**, 230 (1998)
- [58] D. von Harrach, private communication
- [59] HERMES Collaboration, Hermes internal note 97-032, DESY, 1997